

Electroinduced magnetic bubble domain nucleation

Daria Kulikova*, Timur Gareev, Elena Nikolaeva, and Alexander Pyatakov

Physics Department, M.V. Lomonosov Moscow State University, Moscow, Russia

Abstract. The magnetoelectric properties of micromagnetic structures in iron garnet films manifest themselves in electrically induced displacement of domain walls and magnetic bubble domains nucleation. In this paper we found the condition of the electrically induced bubble domain nucleation in terms of critical electric field, magnetic bias and temperature. The collapse of magnetic bubble domain under the action of electric field pulse is also demonstrated.

1 Introduction

The development of information technologies requires continuous search, synthesis and research of new materials allowing new physical principles for storing and recording information. Since the beginning of this century, interest for magnetoelectric materials and multiferroics [1, 2] has been increasing. Magnetoelectric properties can be manifested both in materials with a certain type of crystallographic symmetry and in materials with spatial modulation of the magnetization vector [2]. An example of a magnetic structure with magnetization modulation possessing electric polarization is a Neel-type domain wall [3].

The displacement of the domain wall in an iron garnet film with a crystallographic orientation (210) under the action of an inhomogeneous electric field of the tip electrode was experimentally demonstrated in [4]. This phenomenon is explained by the presence of electrical polarization of the domain wall: the effect is of magnetoelectric nature.

Later it was experimentally shown [4, 5] that the displacement of the domain wall in an inhomogeneous electric field can be increased by applying an in-plane magnetic field.

At the same time I.E. Dzyaloshinskii theoretically predicted the generation of a micromagnetic inhomogeneity from a single domain state by a non-uniform electric field [6]. Later the effect of an electroinduced nucleation of magnetic bubble domain in iron garnet film was observed [7].

In this paper the nucleation of the magnetic bubble domains in iron garnet films depending on external conditions is studied. We also present results on the dynamic collapse of bubble domains under the electric field action.

2 Experiment

2.1. Scheme of experiment

For the experiment the sample with strong magnetoelectric effect previously observed in [1] was chosen. It was $(\text{BiLu})_3(\text{FeGa})_5\text{O}_{12}$ garnet film grown by liquid-phase epitaxy on (210) $\text{Gd}_3\text{Ga}_5\text{O}_{12}$ substrate. In this sample the magnetization direction does not coincide with the normal to the film. The thickness of the substrate is 0.5 mm. The saturation magnetization is $4\pi M_s = 62$ Gs. A stripe domain structure is formed along the $[\bar{1}20]$ direction in the zero external magnetic fields. The period of the domain structure is about 29 μm .

The general scheme of the experiment is shown in Fig.1(a). To create electric field pulses we used a molybdenum wire as a tip electrode with a diameter of about 10 μm touching the surface of the film. The voltage was applied to the electrode by a high-voltage source.

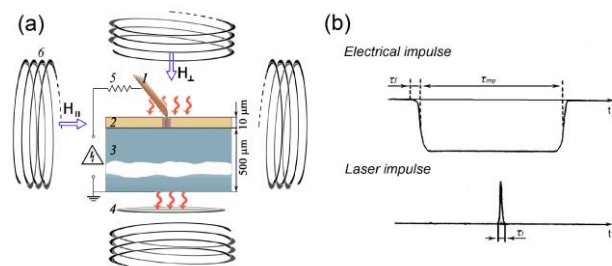


Fig.1. (a) The scheme of the experiment. 1 – tip electrode, 2 – iron garnet film, 3 – substrate, 4 – optical system of the microscope, 5 – ballast resistor, 6 – the coil system. (b) Negative electrical impulse from the generator and the laser impulse.

By supplying a voltage of 500 V to the wire we can obtain electric field strength up to 1 MV / cm. At the same time the voltage jump is enough sharp to nucleate bubble domain (time of charge is about 100 μs). To limit

* Corresponding author: dp.kulikova@physics.msu.ru

the effects of currents of charging, discharging and leakage we used a ballast resistor of 10 MΩ.

According to the Fig.1, the sample was placed between two pairs of coils which created external magnetic bias fields: applied both in the plane of the iron garnet film (H_{\parallel}) and perpendicular (H_{\perp}) to it.

The visualization of the micromagnetic structure was realized with the magneto-optical Faraday effect. The image was recorded using a CCD camera.

To study the dynamic characteristics of the bubble domain generation the high-speed photography technique was used.

The signal of a sequence of rectangular pulses of the electrical voltage was applied to the electrode from the generator. Pulse time is $\tau_{\text{imp}} = 800$ ns and a rise time is $\tau_r = 50$ ns (Fig.1(b)).

The laser pulse duration is $\tau_l = 10$ ns (Fig.1(b)), its start is synchronized with the start of the electric pulse generator. Varying the time delay between field and laser pulses enabled us to observe the consecutive position of domain and thus investigate its dynamics.

2.2 Results of the experiment

In [7] we first demonstrated the generation of the magnetic bubble domain under the action of non-uniform electric field.

We observed the bubble domain generation for two directions of the in-plane magnetic field: along the $[\bar{1}20]$ and $[001]$ directions. The experimental results described below are presented for the in-plane magnetic field along the $[\bar{1}20]$ direction.

The collapse of the stripe domain structure of the iron garnet film occurs at magnetic field about $H_{\parallel} = 50$ Oe. For the further increase of the field H_{\parallel} we use the magnetic field H_{\perp} which is oriented perpendicularly to the film surface. (Fig.2).

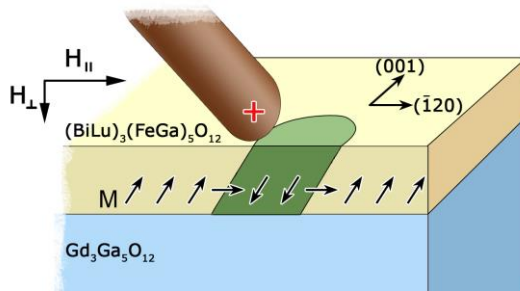


Fig.2. The schematic distribution of the magnetization in the iron garnet film with crystallographic orientation (210).

Magnetic fields of certain values were applied in order the sample was in the single domain state near the transition boundary into a state with a stripe domain structure. When the in-plane magnetic field is oriented along the $[\bar{1}20]$ direction, the values of H_{\parallel} and H_{\perp} were equal to 200 and 70 Oe, respectively. When a positive voltage was applied to the tip electrode over a critical value, the bubble domain nucleation occurred.

The magneto-optical images of the domain structure illustrating the process of the bubble domain nucleation are shown in Fig 3. Initially the sample was homogeneously magnetized (Fig.3(a)). When the positive voltage was applied to the tip, the bubble domain was blown by it (Fig.3(b)). After the voltage was switched off the domain detached from the electrode and decreased in size (Fig.3(c)).

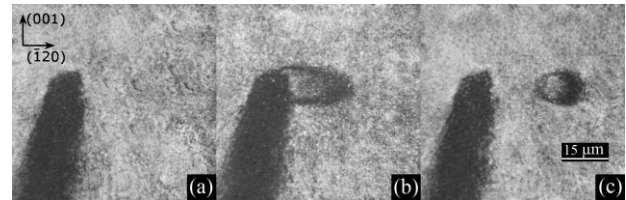


Fig.3. Magneto-optical images of the nucleation of the magnetic bubble domain at $H_{\parallel} = 200$ Oe, $H_{\perp} = 70$ Oe. (a) Tip electrode touches the surface of the film, which is in single domain state. (b) The voltage is switched on, the nucleation of the domain occurs. (c) The bubble domain detaches from the tip when the voltage is switched off.

The nucleation of magnetic bubble domains occurs only in electric fields above some critical value. In its turn the critical voltage depends on the magnitude of the bias magnetic field. The established dependence of the critical voltage on the strength of the magnetic bias field is shown in the Fig 4. In the green area of the magnetic and electric fields (below the curve) the sample is homogeneously magnetized and no nucleation of the domain occurs. In the white area of fields on the graph (above the curve) there is observed both a homogeneously magnetized state and the stripe structure of the sample and also it is possible to generate magnetic bubble domain by electric field. The measurements were carried out at a fixed temperature of the system ($t = 47^{\circ}\text{C}$).

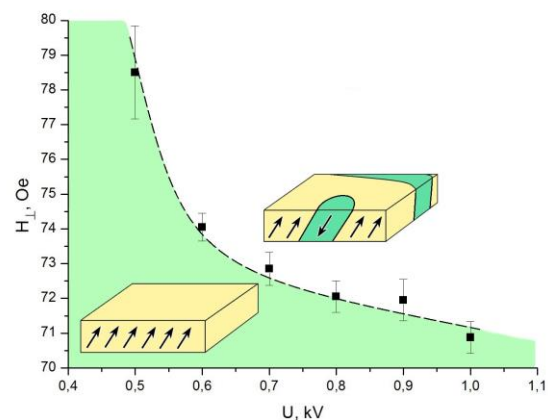


Fig.4. Dependence of the strength of the magnetic bias field on the critical voltage on the electrode.

With an increase of the temperature of the system the minimal magnetic field (which is necessary for the nucleation of the domain) decreases. In Fig.5 it is shown the dependence of the critical magnetic field on the

temperature at fixed values of electric voltage on the electrode $U = 700 \text{ V}$ and of magnetic in-plane field $H_{\parallel} = 200 \text{ Oe}$. Above the curve, there is a possibility of nucleation of bubble domains, below the curve - no. This indicates that the phase diagram in Fig.4 goes "down" when the temperature rises.

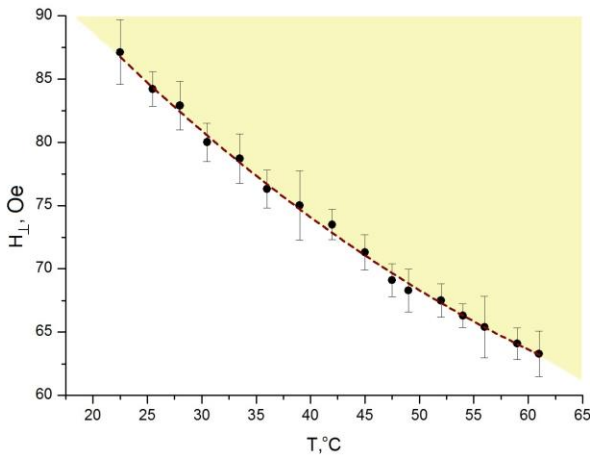


Fig.5. Dependence the critical magnetic bias field on the temperature of the system. $H_{\parallel} = 200 \text{ Oe}$, $U = 700 \text{ V}$.

We also investigated the collapse of the bubble domains under the action of a negative electric field pulse by the method of high-speed photography.

The magnetic bubble domain is generated at the rear front of the negative voltage pulse. Because the repetition period of electric pulses exceeds the width of the front, the domain nucleation process is completed before the next potential change at the electrode occurs. Using this technique we got magneto-optical images of the domain collapse on the forefront of the negative voltage pulse from the generator at different moments of time (Fig.6). The size of the domain decreases with time. At about 350 ns it collapses and the sample is turning to a homogeneously magnetized state again.

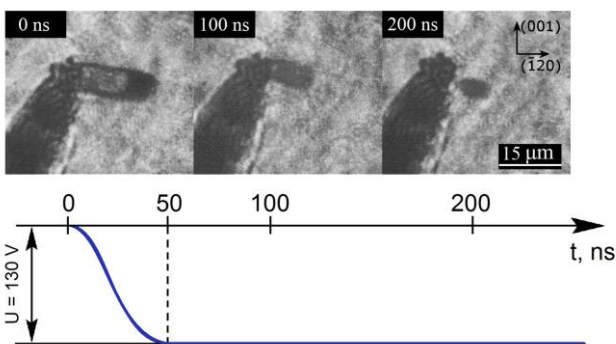


Fig.6. Magnetic bubble domain collapse dynamics in negative electric pulse with an amplitude $U = 130 \text{ V}$.

In Fig.7 it is presented the graph of the dependence of the bubble domain major semiaxis on time. Using the linear fitting it was determined the velocity of the bubble domain walls under the action of electric field. The value of it is about 50 m / s .

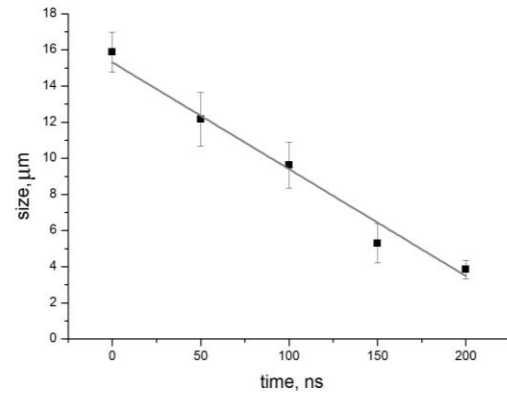


Fig.7. Bubble domain size on time dependence. $H_{\parallel} = 200 \text{ Oe}$, $H_{\perp} = 70 \text{ Oe}$.

Conclusions

We have determined the conditions for bubble domain generation (critical values of external magnetic fields, electric field and their dependence on temperature). It was experimentally demonstrated that bubble domain can be both generated and collapsed under the action of an electric field.

Work was supported by RFBR grants ## 16-02-00494, and 16-29-14037_ofi_m.

References

1. W. Eerenstein, N.D. Mathur, J.F. Scott, *Nature*, **442**, 759 (2006)
2. A.P. Pyatakov, A.K. Zvezdin, *Phys. Usp.*, **55**, 557 (2012)
3. V.G. Bar'yakhtar, V.A. L'vov, D.A. Yablonskii, *JETP Letters*, **37**, 673 (1983)
4. A.P. Pyatakov, A.S. Sergeev, E.P. Nikolaeva, T.B. Kosykh, A.V. Nikolaev, K.A. Zvezdin, A.K. Zvezdin, *Phys.Usp.*, **58**, 981 (2015)
5. A.P. Pyatakov, D.A. Sechin, A.S. Sergeev, A.V. Nikolaev, E.P. Nikolaeva, A.S. Logginov, A.K. Zvezdin. *Europhysics Letters*, **93**, 17001 (2011)
6. I. Dzyaloshinskii, *EPL*, **83**, 67001 (2008)
7. D.P. Kulikova, A.P. Pyatakov, E.P. Nikolaeva, A.S. Sergeev, T.B. Kosykh, Z.A. Pyatakova, A.V. Nikolaev, A.K. Zvezdin, *JETP Lett.*, **104**, 197 (2016)